IOP Conf. Series: Materials Science and Engineering **292** (2018) 012042 doi:10.1088/1757-899X/292/1/012042

Simulation of the temperature field distribution in medium-voltage vacuum interrupter and experimental verification

W Sun[1, 4], H L Liu[2], Y G Cai[2], Y L Li[3], H Y Zhou[1], Y Zhou[1]

[1] Electric Power Research Institute of State Grid Heilongjiang Electric Power Company Limited, Harbin 150030
[2] State Grid Heilongjiang Electric Power Company Limited, Harbin 150090
[3] State Grid Heilongjiang Electric Power Equipment and Materials Company, Harbin 150000)

[4] E-mail: sunwei19850525@163.com

Abstract: The temperature field distribution in the medium-voltage vacuum interrupter decides the thermal stability of it. In this paper, the simulation model of a kind of 12kV/3150A/40kA medium-voltage vacuum interrupter is constructed, and conductive bridge model is used. This paper simulates current contraction and Joule heating between contacts, and solves relevant problems using the function of the thermal-electrical coupling in the finite element software ANSYS. Steady-state temperature rise of vacuum interrupter at rated current and transient temperature rise of vacuum interrupter at short-time withstand current are calculated. Influence of the contact situation on vacuum interrupter temperature rise is analyzed. Steady-state temperature rise experiments for the interrupter are carried out, and experiment results verify the accuracy of simulation results. The results are useful in the designing and optimizing of medium-voltage vacuum interrupter.

1. Introduction

Electric current passes through a conductor of a circuit breaker, and heat is generated as a result during operation of the vacuum circuit breaker. A part of generated Joule thermal energy dissipates in the surrounding medium, while the remaining part heats the vacuum circuit breaker, thereby leading to temperature rise of the circuit breaker. Contact fusion welding may be caused in severe case. In the paper, the conductive bridge model is introduced to simulate current contraction and Joule heating among contacts. The thermal-electrical coupling function of finite element analysis software ANSYS is applied for solving temperature fields in the medium-voltage vacuum interrupter. The steady-state temperature rise of vacuum interrupter samples under uninterrupted duty at rated current of of 3150A is calculated. The influence of contacting condition among contacts on temperature rise of arc extinguish chambers is analyzed. The accuracy of the simulation results is verified through steady-state temperature rise experiments. Finally, the thermal stability of vacuum interrupter samples at short-time withstand current of 40000A and conduction time of 4s is simulated.

2. Establishment of temperature field simulation model

There were three heat transfer methods for medium-voltage vacuum circuit breakers: heat conduction, heat convection and heat radiation. Heat was transferred to external connectors of arc extinguish chamber and external medium thereof through heat conduction in the vacuum interrupter due to the

vacuum state in the arc extinguish chamber, no convection with outside air, and weak radiation[1]. Therefore, heat conduction dissipation was considered only in the vacuum interrupter when the temperature fields in the medium-voltage vacuum interrupter were simulated. However, three heat transfer modes of heat conduction, heat convection and heat radiation were considered aiming at external connectors and busbars of the arc extinguish chamber, wherein two heat transfer modes of heat convection and heat radiation were unified through surface coefficient of heat transfer, thereby reaching the purpose of simplifying calculation.

Therefore, internal 3D heat conduction equation of steady-state medium-voltage vacuum interrupter is shown in equation 1[2]:

$$\lambda(\frac{\partial^2 T}{\partial x^2}+\frac{\partial^2 T}{\partial y^2}+\frac{\partial^2 T}{\partial z^2})=-q \tag{1}$$

Internal 3D heat conduction equation of transient medium-voltage vacuum interrupter is shown in equation 2:

$$\rho c(\frac{\partial T}{\partial t})+\lambda(\frac{\partial^2 T}{\partial x^2}+\frac{\partial^2 T}{\partial y^2}+\frac{\partial^2 T}{\partial z^2})=-q \tag{2}$$

In the temperature：

T ——temperature /K;

λ ——heat conductivity coefficient/ $\mathrm{W\cdot m^{-1}\cdot K^{-1}}$;

q ——energy generated in per unit volume/ $\mathrm{W\cdot m^{-3}}$;

ρ —— material density/ $\mathrm{kg\cdot m^{-3}}$;

c ——specific heat capacity/ $\mathrm{J\cdot kg^{-1}\cdot K^{-1}}$;

t ——time/s;

x,y,z——rectangular coordinates;

Figure 1 shows the calculation model of temperature fields in the medium-voltage vacuum interrupter. In the paper, software Pro/Engineer was applied to establish a simulation model for calculating the temperature field in the vacuum interrupter according to the kind of 12kV/3150A/40kA medium-voltage vacuum interrupter in order to ensure the accuracy of the calculation results.

The temperature field calculation model was mainly composed of an incoming line terminal busbar, an incoming line terminal socket, a static terminal heat radiator, a static conducting rod, a static terminal contact, a dynamic conducting rod, a dynamic terminal contact, a dynamic terminal heat radiator, a leading-out terminal socket and a leading-out terminal busbar, wherein the incoming line terminal busbar and the leading-out terminal busbar were 3000mm long, 100mm wide and 30mm high.

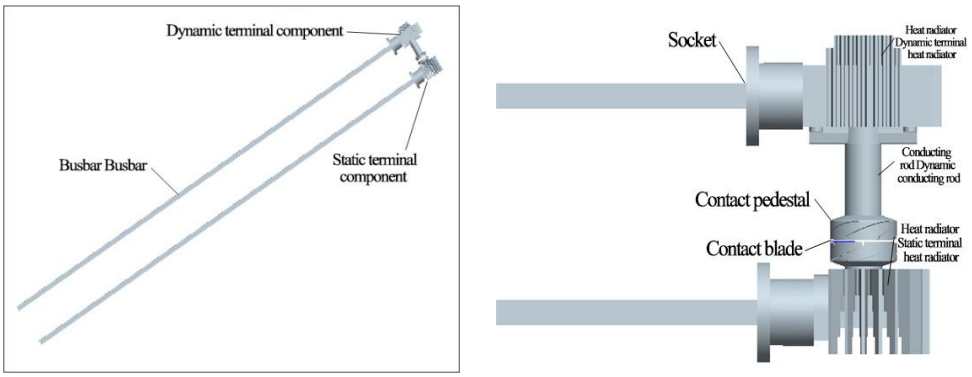

Figure 1. Calculation model of temperature fields in the medium-voltage vacuum interrupter.

Generally speaking, the seemingly smooth contact surface was actually bumpy. Dynamic and static contacts contacted actually in some protrusion points. The contact points were called conductive spots. When the electric current passed through the contact point of the contacts, the current line contracted, thereby increasing the current path near the conductive spot, decreasing the effective conductive

interface, and producing contact resistance. It was usually assumed that there was only one conductive spot between the dynamic contact and the static contact, or all conductive spots formed one large conductive spot in the center position between the dynamic contact and the static contact aiming at general engineering application. In the paper, it was assumed that there was a cylinder in the center of the dynamic contact and the static contact (namely conductive bridge model) for connecting the dynamic contact and the static contact. Figure 2 shows the conductive bridge model.

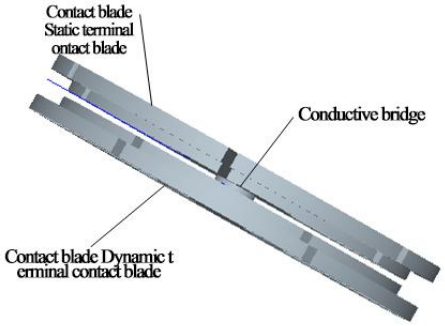

Figure 2. Conductive bridge model.

The material properties of the conductive bridge were the same as the contact material. The radius r of the conductive bridge was calculated from the Holm formula. In the paper, the contact force was 3858N, and the Brinell hardness of the contact material (CuCr50) was 128HB. The contact coefficient of the contact surface was 0.6, therefore the radius r of the conductive bridge was 4mm. The contacts were almostly closed, and the distance was little. Therefore, the height of the conductive bridge was 0.2 mm in the following simulation.

$$r = \sqrt{\frac{F}{\pi \xi H}} \tag{3}$$

In the formula:
F——contact force;
H—— material hardness;
ξ—— contact surface contact coefficient; it is generally 0.3~0.6.

3. Setting of material properties and boundary conditions

Corresponding material properties were set aiming at all parts after the establishment of the model, wherein the conducting rod, contact pedestal, busbar and socket were made of pure copper. The contact support was made of stainless steel. The contact blade was made of CuCr50. The heat radiator was made of aluminum. Table 1 shows the material properties for the model.

Table 1. Material properties of model.

Model name	Material name	Heat conductivity/ $W \cdot m^{-1} \cdot K^{-1}$	Material $/\Omega \cdot m$
Conducting rod	Copper (Cu)	400	$1/5.8\times10^{-7}$[3]
Contact pedestal	Copper (Cu)	400	$1/5.8\times10^{-7}$
Busbar	Copper (Cu)	400	$1/5.8\times10^{-7}$
Socket	Copper (Cu)	400	$1/5.8\times10^{-7}$
Heat radiator	Aluminum (AI)	217	2.7×10^{-8}
Contact support	Stainless steel	15.2	$1/1.1\times10^{-6}$
Contact blade	CuCr50	330	$1/1.41\times10^{-7}$ [4]

Setting of boundary conditions: two end faces of the incoming line terminal busbar and the leading-out terminal busbar were respectively selected as inlet surface and outlet surface of current. The experiment was carried out in a relatively closed temperature rise laboratory. No external airflow entered into the laboratory. The thermal radiation influence was very low. Therefore, heat conduction was the primary heat dissipation method. Busbar and a part of dynamic and static terminal sockets formed convection and heat radiation with outside air. The heat radiation coefficient was the highest. In addition, the busbar was coated with an insulation coating as thick as 0.3mm (alkyd paint). The heat conductivity coefficient of the insulation coating material was generally about 0.2 $W/m^2 \cdot K$. The heat conductivity coefficient of metal was 12~400 $W/m^2 \cdot K$. The integrated heat dissipation coefficient of the busbar and a part of dynamic and static terminal sockets was set as 0.3 $W/m^2 \cdot K$. The other part of the static terminal socket and the heat radiator were semi-closed in the insulating sleeve. The heat radiation coefficient was relatively low. The heat conductivity coefficient of plastic was 0.09 ～ 0.33 $W/m^2 \cdot K$, and the heat conductivity coefficient of air was 0.025～0.035 $W/m^2 \cdot K$. The integrated heat radiation coefficient of the other part of the static terminal socket and the static terminal heat radiator was set as 0.2 $W/m^2 \cdot K$ according to weighted average calculation. The other part of the dynamic terminal socket, the dynamic terminal heat radiator and a part of dynamic conducting rod were completely closed in the insulating sleeve. The heat radiation coefficient was the lowest. The integrated heat radiation coefficient of the three parts was set as 0.001 $W/m^2 \cdot K$ according to weighted average calculation. The remaining part of the calculation model was completely closed in the vacuum interrupter for adiabatic treatment. Steady state temperature field: the input current was the rated power frequency current, the effective value was 3150A, the environment initial temperature was set as 18℃. The input current of the transient temperature field was short-time withstand current: the effective value of the input current was 40000A. The initial temperature was the steady state temperature of the vacuum interrupter.

4. Calculation results of steady-state temperature field and experimental verification

4.1. Calculation results of steady-state temperature field

3D finite element analysis software ANSYS was used. Temperature fields of the medium-voltage vacuum interrupter were simulated through direct coupling of electric fields and thermal fields. The temperature field calculation model is calculated according to material properties and boundary conditions introduced in section 2. The current density distribution of the vacuum interrupter was obtained as shown in figure 3.

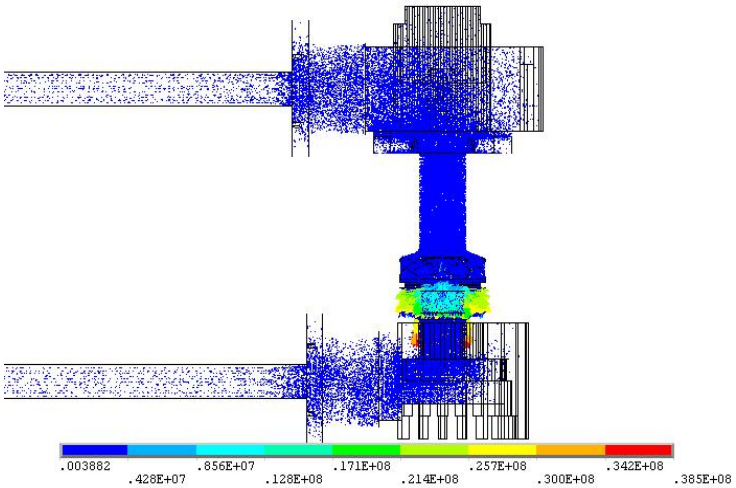

Figure 3. Current density distribution of vacuum interrupter.

Figure 3 shows that the current density distribution of the vacuum interrupter was uneven and there was greater difference among different parts. The current density of the conductive bridge was the largest due to current contraction, and the maximum value was $3.85e^{9}\mathrm{A/m^2}$. The current density of other parts was much smaller compared with the current density of the conductive bridge. It was obvious that the Joule heat caused by the contact resistance between the dynamic and static contacts was the main heat source of the vacuum interrupter.

The temperature field calculation model was calculated according to the previous conditions for obtaining the steady-state temperature field distribution of the vacuum interrupter shown as shown in figure 4.

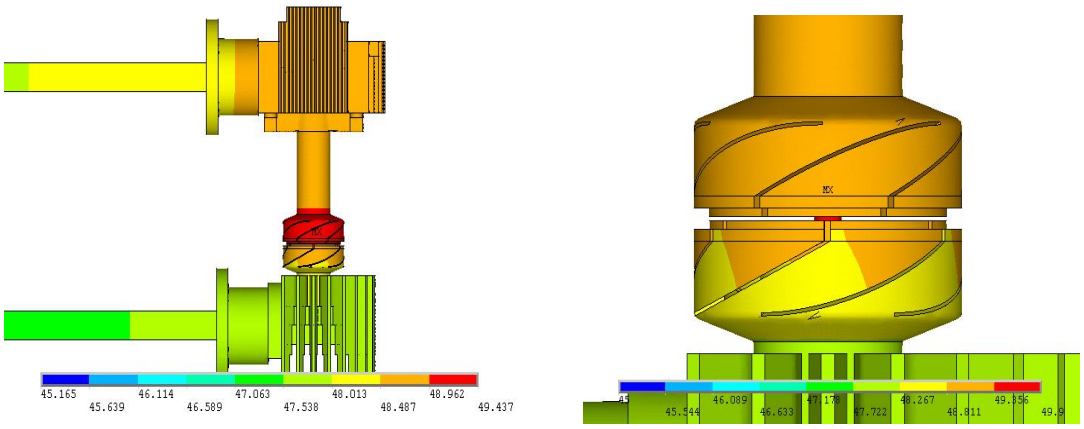

Figure 4. Nephogram of the steady-state temperature rise of the vacuum interrupter.

It is discovered in the figure that the maximum temperature rise value appeared in the conductive bridge part of the vacuum interrupter, which was followed by the temperature rise value of the dynamic contact and the static contact. The temperature rise value of the incoming line terminal busbar and the leading-out terminal busbar was the lowest. The reason is shown as follows: the contact resistance is the main heat source of the vacuum interrupter. The temperature rise value of the part was the highest. The incoming line terminal busbar and the leading-out terminal busbar were relatively far away from the conductive bridge. They formed convection heat dissipation with high convection coefficient. Therefore, its temperature rise value is lower than that of other parts.

The maximum allowable temperature is 90 ℃ in the contact of the AC high-voltage electric appliance under vacuum environment according to the national standards. The maximum temperature value of the vacuum interrupter during long-term work is 67.9 ℃ (ambient temperature of 18 ℃). Therefore, the steady-state temperature value of the vacuum interrupter is consistent with national requirements.

4.2. Experimental verification of steady-state temperature rise of medium-voltage vacuum interrupter

The simulation results should be experimented and tested in order to verify the accuracy of the simulation results. There were usually two methods for testing the temperature field distribution of the vacuum interrupter: the thermocouple method and the infrared camera method [5]. In the paper, a thermocouple was adopted for temperature rise experiment on the selected measurement points according to related national standard of high voltage switch electric appliances.

4.2.1. Experimental content. The experiment was carried out in the temperature rise laboratory. The temperature rise laboratory was not affected by sunlight or other heat radiation. No outside air flowed into the laboratory. The capacity of the temperature rise laboratory was sufficient to ensure normal natural airflow around experiment test object and uniform temperature.

Criteria of temperature rise experiment stability: it was determined that the test object has reached steady-state temperature rise when the temperature rise value change was smaller than 1℃ in one of five measurement points. Figure 5 shows the general circuit diagram of the temperature rise experiment.

Figure 5. General circuit diagram of temperature rise experiment.

Determination of thermocouple measurement point position: measurement points can not be set in the vacuum interrupter due to limitation of experimental conditions. Therefore, measurement points are respectively set in five positions for measuring temperatuer rise, including 'incoming line terminal', 'leading-out terminal', 'static terminal flange', 'static terminal cooling fin' and 'static leading-out terminal'.

4.2.2. Experiment results and analysis. Figure 6 shows the comparison diagram of calculated values and measured values in the measurement points. It is discovered in the figure that the calculated values of five measurement points were respectively 48.52℃, 47.761℃, 47.7℃, 47.833℃ and 48℃. The measured values were respectively 47.64℃, 47.6℃, 45.7℃, 45.02℃ and 48.47℃. The uncertainties between the calculated values and the measured values were respectively: 0.34%, 1.85%, 4.38%, 6.2% and 0.97%. The calculated values and the measured values of the measurement points were basically consistent mutually. However, there was still certain difference between the calculated values and the measured values in the measurement points mainly because the conductive bridge model was different from the actual contacting condition. Model simplification, comprehensive heat transfer coefficient and selection of material parameters also had certain influence on the simulation results.

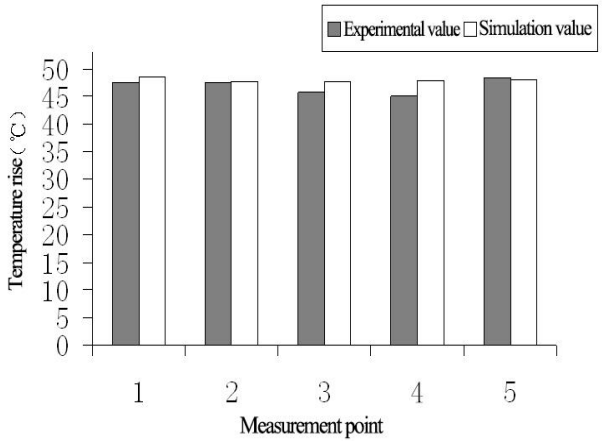

Figure 6. Calculated value and measured value of measurement point.

Another two groups of temperature rise experiments were carried out respectively for comparison: flexible coupling was respectively added in the incoming line terminal and leading-out terminal. Power frequency current with effective value of 3150A was input into the incoming line terminal. The experimental circuit was shown in figure 7. Flexible coupling was not added in the incoming line terminal and leading-out terminal. Power frequency current with effective value of 2000A was input into the incoming line terminal.

Figure 7. General circuit diagram when flexible coupling was added into terminal.

The experiment results of the above two groups of temperature rise experiments were compared with the steady-state temperature rise results of the test objects at rated current. The temperature rise experiment results of the measurement point in the 'leading-out terminal' was adopted as an example. The temperature rise change with time in the 'leading-out terminal' measurement point was concluded as figure 8.

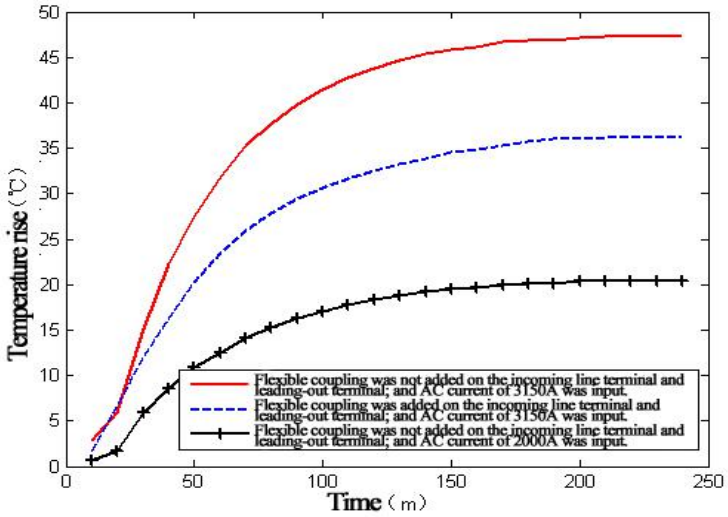

Figure 8. Temperature rise change with time in the 'leading-out terminal' measurement point.

The above figure shows that the temperature rise value of the test object was increased rapidly within short time after current was input into the experiment test object. However, the temperature rise value of the test object tended to be gentle. The test object reached the steady-state temperature rise value about 4 hours later. The steady-state temperature rise value of the experiment test object was lowered by 10℃ or so when flexible coupling was added on the incoming line terminal and leading-out terminal. The convection of the experiment test object and the outside world was enhanced since the contact area between the experiment test object and the external environment was increased by the flexible coupling, which was beneficial for heat dissipation of the experiment test object. The steady-

state temperature rise value of the experiment test object was decreased greatly when power frequency current with effective value of 2000A was input into the incoming line terminal. The steady-state temperature rise value was decreased by 27.23℃. It was obvious that the experiment current has relatively high influence on steady-state temperature rise of the vacuum interrupter.

4.3. Influence of conductive bridge radius on temperature field distribution

The contacting condition among the contacts was mainly embodied in the dimension of the conductive bridge model, namely diameter and height. Changes of conductive bridge size meant changes of contacting conditions. The radius of the conductive bridge was mainly determined by contact contacted pressure, surface contacting condition and the Brinell hardness of contact materials [6]. Surface contacting condition and the Brinell hardness of contact materials were constant values. However the contacts were almostly closed, and the distance was little. Therefore, the influence of contact force on the steady-state temperature field in the medium-voltage vacuum interrupter can be concluded through changing the radius of the conductive bridge.

The height of the conductive bridge was hereby designed as 0.2 mm, and the radius was changed from 1mm to 10mm in order to study the influence of the conductive bridge radius on the temperature field distribution. The temperature rise change of all parts with the conductive bridge radius was obtained as shown in figure 9.

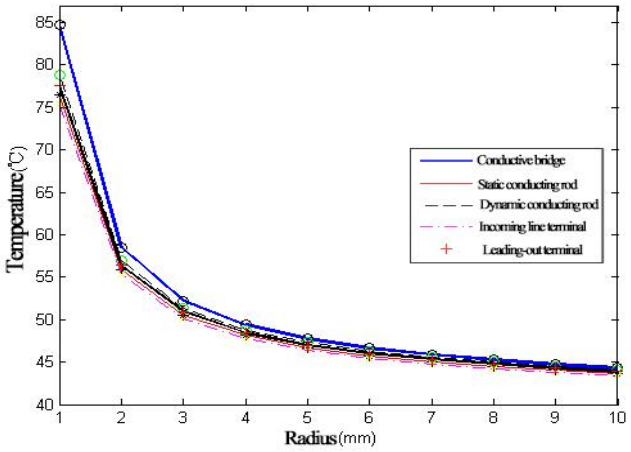

Figure 9. Temperature rise change of all parts with the conductive bridge radius.

Figure 9 shows that the maximum temperature in the arc extinguish chamber was increased from 62.32℃ to 102.78℃ under other constant conditions when the radius of the conductive bridge model was decreased from 10mm to 1mm. The temperature rise value of all parts in the vacuum interrupter was decreased with the increase of the conductive bridge radius. The temperature rise value was changed rapidly with conductive bridge radius at the beginning. The change tended to be slow subsequently because the energy generated by the conductive bridge was $p = I^2 R = I^2 \frac{\rho l}{s} = I^2 \frac{\rho l}{\pi r^2}$, and the change rate was $\frac{dp}{dr} = -\frac{2I^2 \rho l}{\pi r^3}$. In addition, the conductivity bridge was the main heat source, the change rate was relatively high when the radius was relatively small, and the change rate was relatively low when the radius was relatively large as a result. It was obvious that the mechanical burden of the contact was increased only if the contact force was increased merely after the contact force reached certain level. However, the steady-state temperature rise value of the vacuum interrupter can not be decreased prominently. Therefore, the heating problem of the vacuum interrupter can be controlled effectively if the contact force was controlled within certain scope.

5. Calculation results of transient temperature field

The transient temperature field was simulated for analyzing the thermal stability of the medium-voltage vacuum interrupter mainly, which was different from the simulation of the steady-state temperature field. Namely whether the contact of the arc extinguish chamber had fusion welding or not when short-time withstand current passed within short endurance time [7]. In the section, the temperature field calculation model was calculated according to the material properties and boundary conditions introduced in section 2, and the conductive bridge radius was designed as 4 mm. The transient temperature field distribution in vacuum interrupter was obtained. Moreover, the temperature rise value change with time at the maximum temperature point in the vacuum interrupter within 8s under short-time withstand current was studied in the section in order to study the temperature rise value change process with time at the maximum temperature point in the vacuum interrupter and the limit endurance time after short-time withstand current input into the vacuum interrupter. Since the conductive bridge model was relatively small, it can not be clearly displayed in the 3D transient temperature rise nephogram of the vacuum interrupter. Therefore, the transient temperature rise nephogram of the vacuum interrupter at the longitudinal profile was adopted for describing the transient temperature field distribution in the vacuum interrupter in order to describe the transient temperature rise value of the conductive bridge model and the transient temperature field distribution of the vacuum interrupter more clearly. Figure 10 shows the transient temperature rise nephogram of the vacuum interrupter at the longitudinal profile. Figure 11 shows the temperature rise value change with time at the maximum temperature point in the vacuum interrupter within 8s.

Figure 10. Transient temperature rise nephogram of the vacuum interrupter at the longitudinal profile.

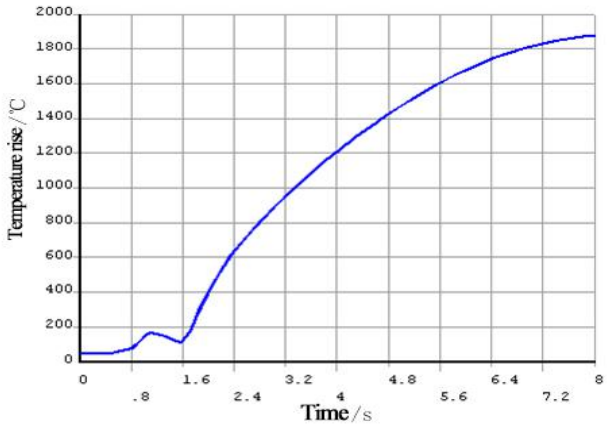

Figure 11. Temperature rise value change with time at the maximum temperature point.

Figure 10 and figure 11 show that the maximum temperature rise value of the temperature field model was 1223℃(environment temperature was set was 18℃) within the short endurance time of 4s

when short-time withstand current (power frequency current with effective value of 40000A) was input into the incoming line terminal. Namely, the maximum temperature value of the vacuum interrupter was 1241℃. Since the contact blade was made of CuCr50, and the melting point of the CuCr50 was 1860℃, the temperature value was far less than the melting point of the contact materials. Fusion welding can not be produced, and thermal stability was satisfied.

Figure 12 also shows that the temperature rise value of the vacuum interrupter was increased rapidly at the beginning of the short circuit. However, the temperature tended to be stable gradually with time. The maximum temperature value of the vacuum interrupter was 1897℃. The temperature value has reached the melting point of the contact, and the contact underwent fusion welding.

6. Conclusion

In the paper, the conductive bridge model was utilized to simulate the current contraction and Joule heating among contacts. Steady-state simulation results showed that the maximum temperature in the arc extinguish chamber was increased from 62.32℃ to 102.78℃ when the conductive bridge radius was decreased from 10 mm to 1 mm. The temperature has been higher than the maximum allowable temperature of the contact of the AC high-voltage electrical appliance (90 ℃). However, the radius of the conductive bridge model was further increased, the temperature field change in the arc extinguish chamber tended to be slow.

Transient simulation results showed that the contact did not undergo fusion welding when short-time withstand current of 40kA passed through vacuum interrupter within the short endurance time of 4s. The thermal stability was satisfied.

In the paper, the steady-state temperature rise experiment was carried out. The results showed that the calculated value of the measurement points was in line with the measured value, and the maximum uncertainty was 6.2%.

Reference

[1] Yu L 2010 Research on development of large current vacuum circuit breaker and key issues *Shenyang University of Technology Press*

[2] Mateev V, Tanev R and Marinova I 2014 Simulation of electric and thermal fields of high voltage interrupter vacuum chamber *Proceedings of XVIII-th International Symposium of Electrical Apparatusand Technologies SIELA* pp 133-136

[3] Cadick J 2012 Predicting the remaining life of vacuum interrupters in the field *Group CBS Alan Seidel*

[4] Liang S H, Fan Z K and Hui R 2000 Research on optimized heat treatment process of CuCr50 contact materials *Transactions of Metal Heat Treatment* chapter **3** pp 66-70

[5] Chen D G, Li X W 2010 Virtual prototype technology of low voltage circuit breaker *Beijing: China Machine Press*

[6] Marinova I and Mateev V 2012 Inverse source problem for thermal fields *Compel International Journal of Computations and Mathematics in Electrical*

[7] Shemshadi A, Akbari A and Bathaee S 2013 A novel approach for reduction of electric field stress in vacuum interrupter chamber using advanced soft computing algorithms *IEEE Transactions on Dielectrics and Electrical Insulation*